

Modeling of gradient composite structures for shielding of microwaves

L. L. Vovchenko, O. V. Lozitsky, I. Y. Sagalianov, L. Y. Matzui, V. V. Oliynyk & V. L. Launets

To cite this article: L. L. Vovchenko, O. V. Lozitsky, I. Y. Sagalianov, L. Y. Matzui, V. V. Oliynyk & V. L. Launets (2016) Modeling of gradient composite structures for shielding of microwaves, *Molecular Crystals and Liquid Crystals*, 639:1, 105-114, DOI: [10.1080/15421406.2016.1255033](https://doi.org/10.1080/15421406.2016.1255033)

To link to this article: <http://dx.doi.org/10.1080/15421406.2016.1255033>



Published online: 14 Dec 2016.



Submit your article to this journal [↗](#)



Article views: 4



View related articles [↗](#)



View Crossmark data [↗](#)

Modeling of gradient composite structures for shielding of microwaves

L. L. Vovchenko^a, O. V. Lozitsky^a, I. Y. Sagalianov^a, L. Y. Matzui^a, V. V. Oliynyk^b,
and V. L. Launets^b

Departments of Physics^a and of Radiophysics, Electronics, and Computer Systems^b, Kyiv National Taras Shevchenko University, Kyiv, Ukraine

ABSTRACT



The simulation of shielding properties of gradient composite structures (g-CMs) nanocarbon-polymer in the frequency range of electromagnetic radiation (EMR) (25.5 – 55.5 GHz) has been implemented in C++ code. The simulation has shown a significant decrease of EMR reflection index (R) and sufficient increase of EMR absorption (A) and shielding efficiency in gradient composite structures with filler concentration growth in the direction of EMR propagation as compared with composite with uniform distribution of nanocarbon filler. The simulated results coincide with the experimental data for the set of the epoxy composites with gradient distribution of 5 wt.% of graphite nanoplatelets.

KEYWORDS

gradient composite materials; graphite nanoplatelets; dielectric permittivity; electromagnetic shielding; reflection and absorption loss

1. Introduction

The differences in structure and morphology of the filler particles (nanotubes, nanoplatelets etc.), alongside with a large aspect ratio, achieving during the formation of the filler, play an important role in the spatial structure and physical properties of heterogeneous composite materials. The electrical conduction process in polymer composites, filled with conductive particles, depends upon a number of parameters, such as filler concentration, particle size and shape, spatial structure, aspect ratio, filler orientation, filler-matrix interactions and processing techniques as governing factors of the electrical properties. By varying the spatial distribution of electroconductive filler in a composite material, we can effectively tune its electronic properties, and hence to control the level of electromagnetic shielding. Frequently used way for achieving the desired level of electromagnetic shielding is to synthesize composite materials with varying electric and magnetic permittivity in different directions relatively to the propagation of the electro-magnetic waves. Multilayer shields with various electrical conductivity and permittivity in different layers [1, 2], gradient-like distributed concentration of filler in the polymer matrix [3, 4, 5, 6, 7] or materials with correlated spatial distribution of anisometric filler particles [8, 9] can be considered as an example. Gradient composite materials (g-CMs) are characterized by a specific 3D distribution of phases and can be superior to homogenous materials composed of the same or similar constituents. The spatial concentration gradient can be produced via sedimentation of filler particles that differ in density from the polymer in its fluid state. A centrifugation technique is the most effective in making a

CONTACT L. L. Vovchenko  vovch@univ.kiev.ua; O. V. Lozitsky  lozitsky@gmail.com
Color versions of one or more of the figures in the article can be found online at www.tandfonline.com/gmcl.

© 2016 Taylor & Francis Group, LLC

graded distribution of filler particles and fabrication of composites with graded properties in the direction of centrifugal force – electrical and thermal conductivity, dielectric permittivity, hardness, Young's modulus, etc [10, 11, 12].

Carbon nanofillers, such as carbon nanotubes, carbon nanofibers and graphite nanoplatelets have been proposed as ideal candidates for the development of next generation composites due to their outstanding properties [13, 14]. Recent studies [15, 16] have presented new results in the investigation of the relationship between the dielectric properties of g-CMs (consisted of multi-walled carbon nanotubes (MWCNTs) and Cyanate ester resin (CE), including the difference in permittivity over a wide frequency range from 1 to 10^9 Hz and the interfacial effect on the dielectric properties. It was found that although conductive networks and electron tunnels may be formed in some regions of the gradient composite, a thorough percolation network isn't achieved in the whole composite. Therefore, the MWCNT/CE g-CMs remain insulators, and the sudden insulator-to-conductor transition, or percolation phenomenon, does not appear. These results confirm a high permittivity of the g-CMs as a consequence of its special dispersion and distribution of nanotubes in the matrix along the direction of thickness instead of the percolation effect.

In [17] it was shown that the combination of impressive permittivity of inorganic particles with good dielectric strength of polymers may result in a high-permittivity polymer-based flexible composites. An attempt has been made to enhance the microwave shielding properties of elastomeric composites by introduction of a magnetic filler (iron particles) concentration gradient along the thickness [18, 19]. Composites having both carbon nanomaterials (graphene, carbon nanotube, etc.) and carbonyl iron particles as filler have also been studied for their EMI SE properties [20, 21].

Utilizing gradient structures as shielding materials opens a wide range of possibilities for tuning the interaction of CMs with EMR, and therefore, the reflection and absorption of electromagnetic shielding materials.

In the present study we have modeled the effect of various filler concentration gradients in CMs on shielding properties and compared the simulated and experimental results for the epoxy g-CMs filled with graphite nanoplatelets. The obtained computer-simulated results allow the prediction of EM properties in polymer-electroconductive filler gradient composites.

2. Experimental section

Gradient distributions of conductive filler in the polymer matrix of epoxy CMs are made by separating the liquid mixture of polymer and disperse filler in the centrifuge. By varying the concentration of filler in the polymer matrix C , the rotational speed ω , centrifugation time t , amount of composite mixture M and its viscosity, CMs can be obtained with different degrees of filler concentration gradient along the selected axis of the sample, from decreasing the concentration along the test-tube height (with a small t) to a sharp separation of filler and polymer in the solution (for large ω and t). The schematic model of obtained concentration gradient is shown in Fig. 1a, 1c.

We synthesized gradient composite structures using epoxy matrix ED20, filled with 5wt.% of graphite nanoplatelets (GNPs) [22]. Graphite nanoplatelets (average diameter 10 μm , average thickness 40 nm) were prepared by ultrasonic dispersing of thermoexfoliated graphite particles in acetone. Centrifuging the liquid GNPs-ED20 mixture, creates particle size (thickness and diameter) and concentration gradients. Four types of CMs ED20–5wt.% GNPs with different GNP distribution gradients, achieved with different centrifuge rotational

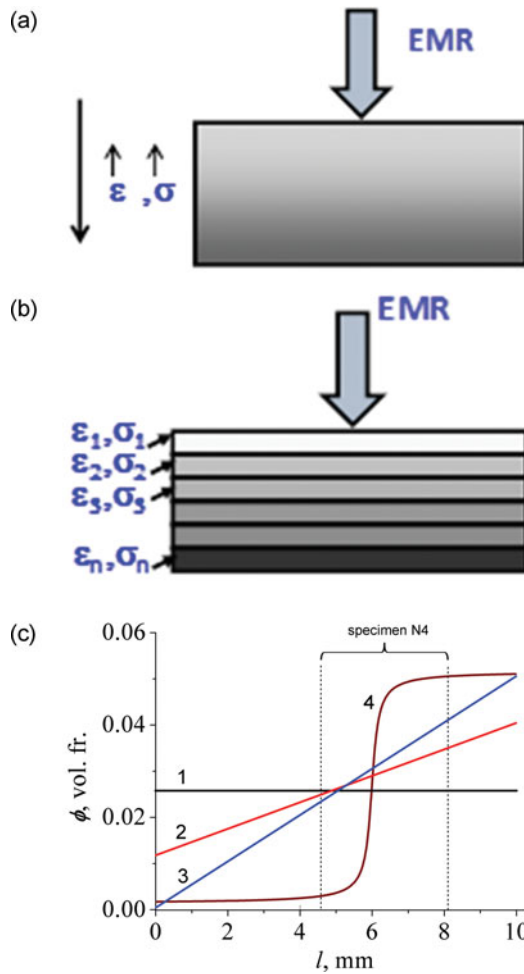


Figure 1. Gradient composite structure polymer-conductive filler (a, b) and difference in filler concentration along the shield width / in the direction of EMR propagation (c): a) gradual increase of filler concentration in the CM; b) CM image in a multilayered structure form; c) 1 — uniform concentration distribution ($m = 1$); 2, 3 — linear concentration gradient, $m = 0.5$ and $m = 0$, respectively; 4 — significant stratification of the CM during long centrifugation with a high rotational speed.

speed: 3000 (1), 4000 (2), 5000 (3) and 6000 (4) spins per minute (samples 1, 2, 3 and 4 with widths of 8.7, 7.7, 11 and 3.5 mm) were prepared. According to [4], under a low spinning time and velocity of the centrifugation, we can observe the formation of a linear concentration gradient — Fig. 1c (curves 1, 2, 3). The increase of centrifugation time and velocity causes a significant stratification of the CM according to Fig. 1c (curve 4). The sample 4 was divided into two parts: one with almost pure epoxy and one with almost pure GNP (Fig. 1c) and for the investigation the part of the sample (with thickness in 3.5 mm) was cut from whole sample as indicated by dashed lines in Fig. 1c. Higher levels of filler particles anisotropy (aspect ratio) provide higher concentration gradients that can be achieved after centrifugation.

Microwave properties such as the reflection loss, absorption loss and transmission index were measured in the frequency range of 25.5–37.5 GHz. The specimens of gradient GNPs-epoxy composites in a form of $7.2 \times 3.4 \times l$ mm³ plates were prepared to analyse the interaction of electromagnetic radiation (EMR) with the studied materials. Such specimen's shape allows totally overlap the cross-section of a rectangular copper waveguides. A P2-65 device

(the equivalent of a microwave network analyzer) was used to measure the transmission coefficient within the 25.5–37.5 GHz frequency range. Voltage measurements of the standing wave ratio (SWR) were used to determine the reflection properties of the studied specimens [22].

3. Results and discussion

3.1. Simulation of shielding properties for gradient composite structures

Composite structures with a gradient distribution of electroconductive filler are characterized by a growth of electrical conductivity in the direction of increasing filler concentration, which is similar to the percolation effect along the width of the sample — the first layers are almost dielectric, while the next ones get larger concentrations of filler, hence, better electrical conductivity. In the case of spatially asymmetric filler particles with a high aspect ratio (graphite nanoplatelets, nanofibers or nanotubes) in gradient composites, we have observed differences in the spatial distribution of filler particles [4], which effectively tune the electrical conductivity of the sample along the thickness of the shield.

During the EMR propagation process we can obtain the reflection R (RL in dB), absorption A and transmission T (SE_T in dB) indexes for monolayer shield using the following relations [23, 24, 25]:

$$A + T + R = 1; R = |r|^2 = |E_r'/E_i|^2; T = |t|^2 = |E_T/E_i|^2 \quad (1)$$

$$RL = 20 \lg |r|; SE_T = 20 \lg |t| \quad (2)$$

where E_i , E_r' , E_T are the electric field strengths of incident, reflected, and transmitted waves, respectively, r is the amplitude reflection index, t is the amplitude transmission index.

In our model calculations, the reflection (R), absorption (A) indexes and shielding efficiency (SE_T) depend mainly on the frequency of EMR wave f , permittivity ε_r' , tangent loss $\tan \delta$ and thickness of the sample (shield) l [26, 27]:

$$r = \frac{(r_{12} - r_{12} \cdot e^{-2\gamma \cdot l})}{(1 - r_{12} \cdot e^{-2\gamma \cdot l})} \text{ and } t = \frac{(1 - r_{12}^2) \cdot e^{-\gamma \cdot l}}{(1 - r_{12}^2 \cdot e^{-2\gamma \cdot l})}, \quad (3)$$

where $r_{12} = (1 - n)/(1 + n)$ is the reflection index on the boundary free space-material; $n = k_z/k_0$ is the complex index of refraction; $k_0 = 2\pi/\lambda_0$ is the wave vector in free space, $\lambda_0 = C_0/f$; λ_0 and f are the wavelength and the frequency; $C_0 = 3 \cdot 10^8$ m/s; $k_z = k_0 \cdot \sqrt{\varepsilon_r^* \mu_r^*}$; $\gamma = i \cdot k_z = \alpha + i\beta$ is the propagation constant of the electromagnetic waves, β is the phase constant, α is the absorption index; $\varepsilon_r^* = \varepsilon_r' - i\varepsilon_r''$ and $\mu_r^* = \mu_r' - i\mu_r''$ are the relative complex permittivity and relative complex permeability of medium, respectively.

For the case of nonmagnetic composite the values of α and β may be described by following expressions:

$$\alpha = \frac{2\pi}{\lambda} \cdot \sqrt{\varepsilon_r'} \cdot \sqrt{0.5 \cdot (\sqrt{(1 + \tan^2 \delta)} - 1)}, \quad \beta = \frac{2\pi}{\lambda} \cdot \sqrt{\varepsilon_r'} \cdot \sqrt{0.5 \cdot (\sqrt{(1 + \tan^2 \delta)} + 1)}, \quad (4)$$

where $\tan \delta = \varepsilon_r''/\varepsilon_r'$.

The calculation of shielding properties in gradient composite structures was implemented using the impedance method in C++ code. The CM was divided into n independent layers ($n = 100$ – 1000), where filler concentration increased in each subsequent layer. This impedance method (described in detail in our previous paper [28]) gives the expressions for

the reflection loss (RL) and transmission (SE_T) by using of recurrent impedance ratios:

$$RL = 20 \lg \left| \frac{(X_n - Z_{n+1})}{(X_n + Z_{n+1})} \right|; \quad (5)$$

$$SE_T = 20 \lg \left(\prod_{j=1}^n \left| \frac{(X_j + Z_j)}{(X_j + Z_{j+1})} \cdot \exp(-\gamma_j l_j) \right| \right) \quad (6)$$

Where Z_j (X_j) — input (output) impedance for j -th layer. Reflection loss RL is calculated for the n -th layer and clearly depends on reflection losses on previous layers. In other words, RL in our calculations is total reflection loss for multilayer composite structure.

For the measurements in rectangular waveguide:

$$\gamma_j = i \cdot k_0 \sqrt{\varepsilon_r' \cdot (1 - i \cdot \tan \delta_j) - \left(\frac{\lambda}{2a}\right)^2} \quad (7)$$

$$Z_j = \frac{Z_0}{\sqrt{\varepsilon_r' \cdot (1 - i \cdot \tan \delta_j) - \left(\frac{\lambda}{2a}\right)^2}} \quad (8)$$

$$X_j = \frac{Z_j(X_{j-1} + Z_j \cdot \tanh(\gamma_j \cdot l_j))}{(Z_j + X_{j-1} \cdot \tanh(\gamma_j \cdot l_j))} \quad (9)$$

where $Z_0 = \sqrt{\mu_0/\varepsilon_0} = 377 \, \Omega$ is the wave impedance of free space, $a=7.2$ mm or 5.2 mm — the inside width of rectangular waveguide.

As an example, we have considered a CM, filled with graphite nanoplatelets in an epoxy polymer matrix with concentration $\phi = 0.047$ vol. fr. (5wt.%). For this type of composites ED20-GNPs we have used the experimental concentration dependencies $\varepsilon_r'(\phi)$ and $\tan \delta(\phi)$ fitted with following approximation functions [28]:

$$\varepsilon_r' = -10.51 + 12.13 \cdot \exp(\phi/0.0284); \quad \tan \delta = -0.15 \cdot (1 - \exp(\phi \cdot 16.505)) \quad (10)$$

The thickness of the gradient sample is $l = 10$ mm. The slope of the filler concentration gradient (in the direction of EMR propagation) was varied by a linear function, dependent on the number of the layer:

$$\phi_i = \phi_0 + \frac{\phi_n - \phi_0}{l} \cdot \frac{l}{n} \cdot (i - 0.5) = \phi \cdot \left(m + \frac{2(1-m)}{n} \cdot (i - 0.5) \right) \quad (11)$$

where $\phi_0 = m \cdot \phi$ is the filler concentration in the first layer; $\phi_n = \phi(2 - m)$ is the filler concentration in the last layer; the value of parameter m varies from 1 (uniform filler distribution) to 0 (maximum allowed linear concentration gradient under given thickness l of the sample).

Computation results of the frequencies dependencies of reflection, absorption and transmission indexes for the CM in cases of increase (direct gradient) and decrease (reverse gradient) concentration gradients depicted in Fig. 2.

As we can see from Fig. 2a, b, for the uniform filler distribution in the sample, the average values of R and A indexes are almost similar (around 0.5). Creation of GNP concentration gradient weakens the EMR through the process of reflection and adsorption of electromagnetic radiation between the layers. The values of R and A strongly depends on the direction of EMR propagation relatively to the concentration gradient: a direct gradient decreases R and increases A in accordance to the slope value, while the inverse gradient causes an

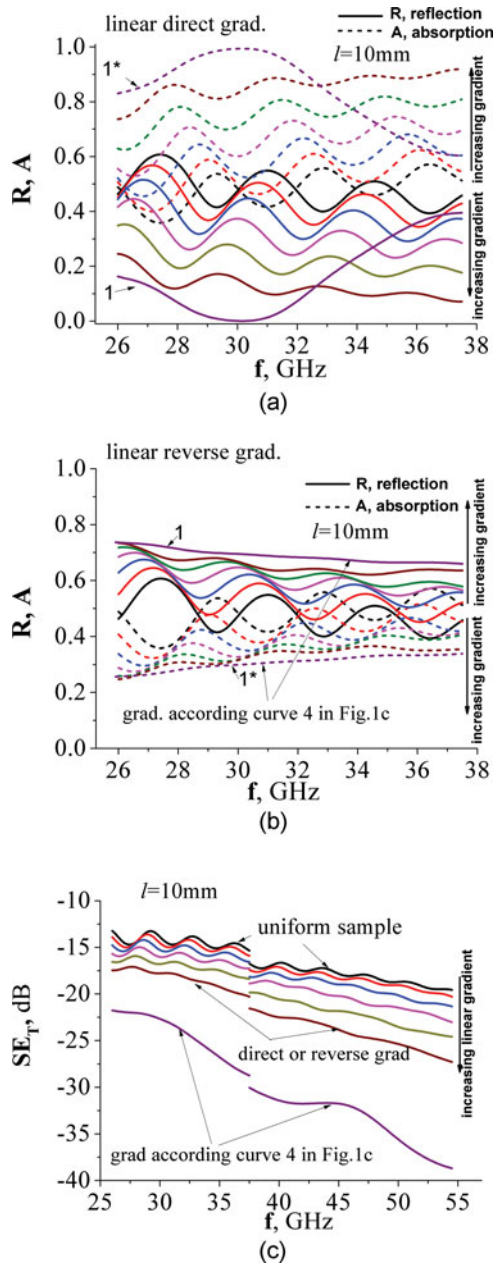


Figure 2. Simulated data on reflection R (solid lines), absorption A (dashed lines) indexes for EMR (a, b) and shielding efficiency SE_T (c) in 5wt.% GNPs-ED20 structures with different linear gradient of GNPs concentrations in direction of EMR propagation and for composite structure with essential stratification of phases (curve 4 in [fig. 1c](#)): a direct gradient in the direction of EMR propagation (a), $m = 1$ — homogeneous sample, and increasing gradient $m = 0.8$; $m = 0.6$; $m = 0.4$; $m = 0.2$; $m = 0$ — maximum concentration gradient (see Eq.(11)); reverse gradient in the direction of GNP concentration decrease (b); curves 1, 1* correspond to stratification of phases in composite.

opposite influence. This behavior of R and A is a clear consequence of minimal (maximal) wave impedance mismatch on the first air-shield boundary and it causes minimal (maximal) values of R and maximal (minimal) values of A , because the biggest part of the EMR is adsorbed in the sample (reflects on the first layer). As we can see from [Fig. 2c](#), shielding

efficiency enhances with gradient slope in the direction of EMR propagation (results in case of reverse gradient usage coincide with results, obtained with direct gradient sample). The maximal EMR shielding efficiency was observed for composite with significant stratification of GNPs and epoxy phases as presented by curve 4 in Fig. 1c.

3.2. Shielding properties of gradient composites graphite nanoplatelets-epoxy resin

Experimentally measured dependencies of reflection R , absorption A indexes and shielding efficiency SE_T on frequency of EMR waves for epoxy CMs with 5wt.% GNPs with different growing concentration gradient slopes are presented in Fig. 3. For comparison, Fig. 3 presents also the theoretical results for shields with different thickness (3.5 and 10 mm) of a homogeneous CM (uniform distribution of GNPs). Figure 4 shows comparative diagrams for reflection R and absorption A indexes at a 27 GHz frequency for both direct and inverse GNP concentration gradient structures in CMs.

As we can see from experimental data (Fig. 4), the reflection R , absorption A and transmission SE_T of electromagnetic radiation in the gradient composite structures change accordingly to our theoretical predictions. For example, increasing the GNPs concentration gradient in the direction of EMR propagation reduces R and increases A . Shielding effectiveness of gradient samples is also significantly enhanced compared to uniform ones. Larger tilt of frequency dependencies for samples 1, 2 and 3 compared with the test sample

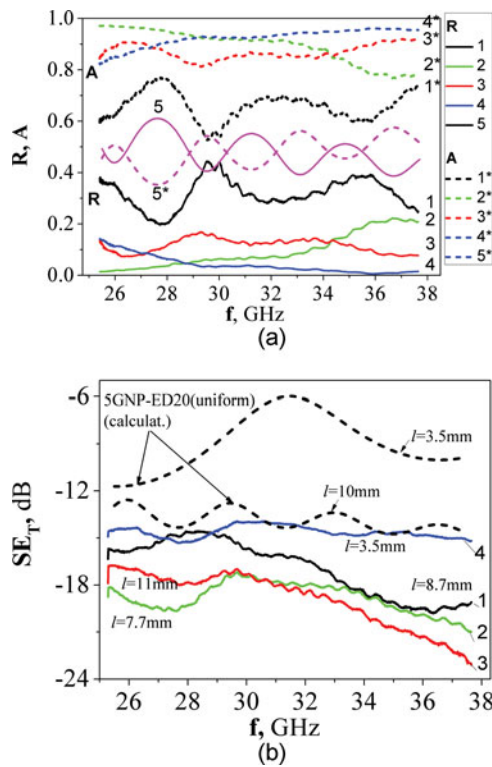


Figure 3. Reflection R (solid lines 1–5) and absorption A (dashed lines 1*–5*) indexes (a) and shielding efficiency SE_T (b) in gradient structures of 5wt%GNP-ED20 during the propagation of EMR in the direction of GNP concentration increase; numbers of the curves coincide with the numbers of experimental gradient samples — 1, 2, 3, 4 and 5, 5* are numerical simulation for CMs with homogeneously distributed GNPs.

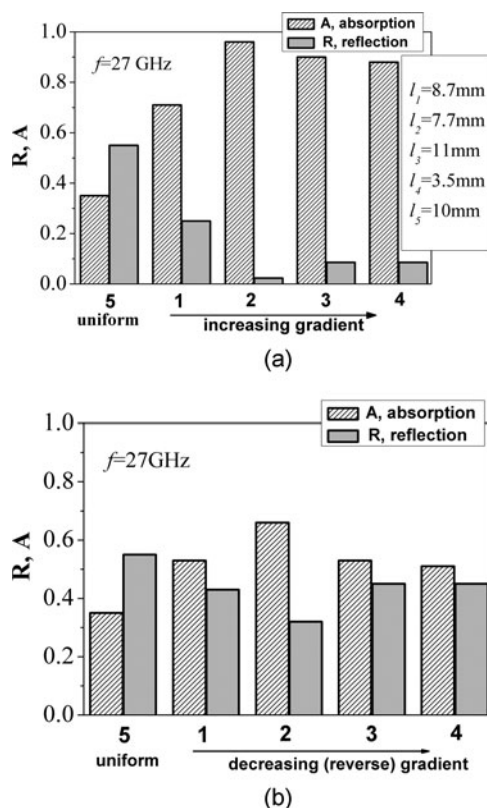


Figure 4. Experimental data on EMR reflection and absorption indexes for gradient composites 5wt.%GNPs-epoxy: a) increasing gradient (direct); b) decreasing gradient (reverse); diagram numbers 1 to 4 coincide with sample numbers, last diagram 5 corresponds to the 5 wt.% GNP-ED20 sample with uniformly distributed GNPs.

5wt.% GNP-ED20 (homogeneous distribution of GNP) and the gradient one (sample 4) usually indicates that a relatively large part of EMR is absorbed in samples 1, 2, 3 due to their greater thickness and different concentrations of GNPs contrary to the part of the electromagnetic radiation that is reflected by the shield.

Thus, as mentioned earlier, thick shields with a non-zero attenuation coefficient α demonstrate an enhancement of the shielding effectiveness with frequency increasing (see Eqs. (2, 3)).

A comparison of EMR reflection R , absorption A and shielding efficiency SE_T (Figs. 5a, b) for several different samples with gradient GNPs distribution has shown good agreement between experimental and theoretical predictions. We assume that some differences between experiment and theory are caused by a more complicated (sub/super-linear) form of the concentration gradient or, by the formation of a solid GNPs layer on the other side of the electromagnetic shield at phase stratification, affecting both absorption and reflection of EMR.

From the analysis of calculated and experimental data we can conclude that the least reflection coefficient and the highest absorption index in g-CMs are a consequence not to a linear concentration gradient, but to the presence of significant stratification in the composite material.

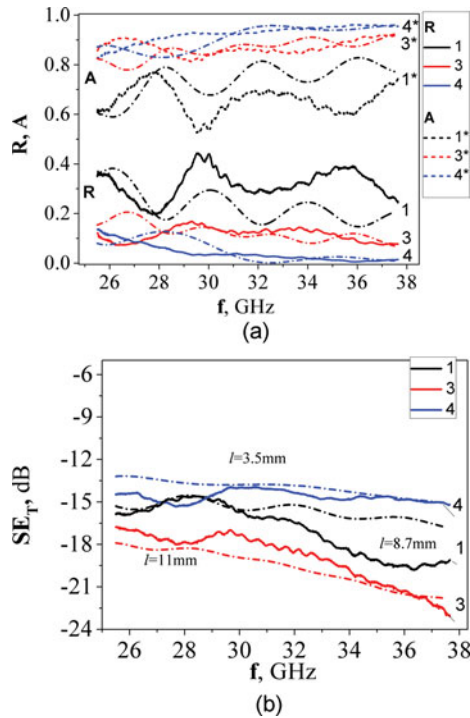


Figure 5. Comparison of the experimental and simulated data on EMR reflection R and absorption A indexes (a) and shielding efficiency SE_T (b) for gradient composites 5wt.%GNPs-epoxy; numbers of curves denote numbers of samples; solid lines are experiment, dash-dotted curves are calculation for CMs with linearly fitted gradient function (sample 1 ($m = 0.2$); sample 3, ($m = 0$) and with concentration gradient on Fig. 1c (curve 4) for sample number 4.

4. Concluding remarks

The modeling of shielding properties of polymer-nanocarbon composites in microwave range (25.5 – 55.5 GHz) has shown a significant decrease of the EMR reflection index (R) and a sufficient increase of EMR absorption (A) in gradient composite structures, as compared to composites with a uniform distribution of nanocarbon filler, where filler concentration increases in the direction of EMR propagation. Simulated results for the reflection and absorption indexes agreed with experimental data for a set of epoxy composites with a 5 wt.% gradient distribution of GNPs. Such changes in EMR reflection and absorption indexes are explained by a decrease of wave impedance mismatch at the first “free space – shielding material” boundary (low concentration of electroconductive filler causes low conductivity and dielectric permittivity), so the larger part of EMR entered into the shield and was absorbed by its material. We have also shown the increase of EMR shielding efficiency (EMR transmission index SE_T) in composite structures with the increase of filler concentration gradient.

The proposed method for designing composite structures with inhomogeneous filler distribution opens new possibilities in tuning the EMR absorption and reflection properties of the composite structures for various electromagnetic applications.

References

- [1] Danlee, Y., Huynen, I., & Bailly, C. (2012). *Appl. Phys. Lett.*, 100, 213105.
- [2] Gargamam, H., Chaturvedi, S. K., & Thakur, A. K. (2012). *Progress In Electromagnetics Research B*, 39, 241.

- [3] Ahankari, S., & Kar, K. K. (2012). *J. Appl. Polym. Sci.*, 25, 3469.
- [4] Klingshirn, C., Koizumi, M., Hauptert, F., Giertzsch, H., & Friedrich, K. (2000). *Journ. of Mater. Sci. Lett.*, 19, 263.
- [5] Stabik, J., Szczepanik, M., Dybowska, A., & Suchon, L. (2010). *Journ. of Achiev. in Mater. And Manufactor. Engineering.*, 38, 56.
- [6] Nigrawal, Archana, Chand, Navin (2014). *American Journ. of Mater. Sci. and Appl.*, 2, 43.
- [7] Udupa, Gururaja, S. Shrikantha Rao, Gangadharan, K.V. (2014). *Procedia Mater. Sci.*, 5, 1291.
- [8] Arjmand, M., Mahmoodi, M., Gelves, G. A., Park, S., & Sundararaj, U. (2011). *Carbon*, 49, 3430.
- [9] Mahmoodi, M., Arjmand, M., Sundararaj, U., & Park, S. (2012). *Carbon*, 50, 1455.
- [10] Tsoira, P., & Friedrich, K. (2003). *Compos. Part A: Appl. Sci. Manuf.*, 34, 75.
- [11] Hashmi, S. A. R., Dwivedi, U. K., Jain, D., Naik, A., & Chand, N. (2005). *J. Appl. Polym. Sci.*, 96, 550.
- [12] Gasik, M. M. (2010). *Int. J. Materials and Product Technology*, 39, 20.
- [13] Morishita, T., Matsushita, M., Katagiri, Y., & Fukumori, K. (2011). *J. Mater. Chem.*, 21, 5610.
- [14] Ahankari, S. S., & Kar, K. K. (2010). *J Appl Polym Sci.*, 115, 3146.
- [15] Wu, H., Gu, A., Liang G., & Yuan, L. (2011). *J. Mater. Chem.*, 21, 14838.
- [16] Wang, B., Liu, L., Liang, G., Yuana, L., & Gu, A. (2015). *J. Mater. Chem. A*, 3, 23162.
- [17] Dang, Z. -M., Yuan, J. -K., Zha, J. -W., Hu, P. -H., Wang, D. -R., & Cheng, Z. -Y. (2013). *Journal of Advanced Dielectrics*, 3, 1330004.
- [18] Gargama, H., Thakur, A. K., & Chaturvedi, S. K. (2016). *J. Alloys Compd.*, 654, 209.
- [19] Raghunandan Sharma, Sandeep S Ahankari, Kamal K Kar, Animesh Biswas and Srivastav K. V. (2015). *Journal of Elastomers & Plastics*. DOI: [10.1177/0095244315620917](https://doi.org/10.1177/0095244315620917).
- [20] Chen, Y., Zhang H. -B., & Huang Y., et al. (2015). *Compos Sci Technol.*, 118, 178.
- [21] Wang, H., Zhu, D., & Zhou, W., et al. (2015). *Ind. Eng. Chem. Res.*, 54, 6589.
- [22] Vovchenko, L., Matzui, L., Oliynyk, V., & Launetz, V. (2010). *Phys. Status Solidi C*, 7, 1260.
- [23] Wang, Z., & Zhao, G. -L. (2013). *Open J. Compos. Mater.*, 3, 17.
- [24] Joo, J., & Lee, C. Y. (2000). *J. Appl. Phys.*, 8, 513.
- [25] Liu, Z., Bai, G., Huang, Y., Ma, Y., Du, F., Li, F., Guo, T., & Chen, Y. (2007). *Carbon*, 45, 821.
- [26] Dhawan, S. K. et al. (2011). In: *Advances in Nanocomposites - Synthesis, Characterization and Industrial Applications*, book edited by Reddy, Boreddy (Eds.), Chapter 19, ISBN 978-953-307-165-7, DOI: [10.5772/14752](https://doi.org/10.5772/14752), 429–481.
- [27] Polyakova, O. N., Tikhonov, V. V., Dzardanov, A. L., Boyarski, D. A., & Gol'tsman, G.N. (2008). *Tech. Phys. Lett.*, 34, 967.
- [28] Sagalianov, I. Yu., Vovchenko, L. L., Matzui, L. Yu., Lazarenko, A. A., Oliynyk, V. V., Lozitsky, O. V., & Ritter, U. (2016). *Mat.-wiss. u. Werkstofftech.*, 47, 263.